JOURNAL OF GEOPHYSICAL RESEARCH, VOL. 89, NO. B7, PAGES 6329–6340, JULY 10, 1984

Reflectance Spectroscopy: Quantitative Analysis Techniques for Remote Sensing Applications

ROGER N. CLARK[1] AND TED L. ROUSH

Planetary Geosciences Division, Hawaii Institute of Geophysics
University of Hawaii

Several methods for the analysis of remotely sensed reflectance data are compared, including empirical methods and scattering theories, both of which are important for solving remote sensing problems. The concept of the photon mean optical path length and the implications for use in modeling reflectance spectra are presented. It is shown that the mean optical path length in a particulate surface is in rough inverse proportion to the square root of the absorption coefficient. Thus, the stronger absorber a material is, the less photons will penetrate into the surface. The concept of apparent absorbance (-ln reflectance) is presented, and it is shown that absorption bands, which are Gaussian in shape when plotted as absorption coefficient (true absorbance) versus photon energy, are also Gaussians in apparent absorbance. However, the Gaussians in apparent absorbance have a smaller intensity and a width which is a factor of $\sqrt{2}$ larger. An apparent continuum in a reflectance spectrum is modeled as a mathematical function used to isolate a particular absorption feature for analysis. It is shown that a continuum should be removed by dividing it into the reflectance spectrum or subtracting it from the apparent absorbance and that the fitting of Gaussians to absorption features should be done using apparent absorbance versus photon energy. Kubelka-Munk theory is only valid for materials with small total absorption and for bihemispherical reflectance, which are rarely encountered in geologic remote sensing. It is shown that the recently advocated bidirectional reflectance theories have the potential for use in deriving mineral abundance from a reflectance spectrum.

INTRODUCTION

The use of remotely obtained spectra of planetary surfaces for geologic studies has increased dramatically in the last decade. Spectral data have been used to identify minerals on the earth and on all the solid surfaces in the solar system as well as composition of atmospheres when present. The reflectance spectrum of a particulate surface is very complex, being affected by the number and type of materials present, their weight fractions, the grain size of each material, and the viewing geometry. Because of the complexity, adequate theories for predicting the light returned (scattered) from the surface have not been precise enough for all applications and conditions. Absorption bands due to electronic transitions, vibrational modes, charge transfer processes, and other processes [e.g., see *Hunt,* 1977] often allow a unique identification of the mineral to be made. However, relating a spectral feature identification to actual mineral abundance is difficult. Thus, the interpretations of reflectance spectra have been made by studying many types of spectra under different conditions such as differing grain sizes or mixtures of various materials. This empirical method sometimes results in confusion of a particular interpretation for the nonexpert and even disagreement among the experts.

Because the current theories have not been shown to be precise enough for all conditions and applications, considerable effort has been undertaken to study many different conditions in the laboratory to derive empirical trends. The near future holds the promise of mapping spectroscopy, where a reflectance spectrum will be obtained of planetary surfaces at many spatial points on the surface. Such techniques can easily produce millions of spectra. Since the scattering theories are complex, their use requires considerable computer time possibly precluding their use on millions of spectra. Thus, the future analysis of spectral data will likely occur at several levels. When large amounts of data are involved, only simple analyses can be practically done, like correlation of a particular mineral with the ratio of data at two different wavelengths. A next level effort might be a search for a particular absorption feature and a derivation of its depth. In some cases, an empirical trend in several parameters derived from laboratory studies might be applied to the data. In the most detailed analysis, a sophisticated scattering analysis might be applied. The degree of accuracy desired in the resulting analysis, and the amount of data to process, will most likely drive the selection of methods to be used.

Although the number of theories for the scattering within a particulate surface and their accuracy appear to be increasing, there will always be a need for laboratory studies to verify, refine, and extend the theories. Since, in most studies, the goal is to determine the composition and physical properties of the surface, the understanding of how photons are scattered from a particulate surface is essential, whatever the analysis method used. In the empirical case, this understanding might be the derivation of absorption band depth as a function of grain size. In the scattering theory case, it might be the determination of grain size and complex refractive index.

It should be noted that scattering theories are often presented in terms of deriving the absorption coefficient (related to the complex refractive index) of the surface material. Once the absorption coefficient as a function of wavelength has been found, the material may be identified by comparison with known mineral absorption data. This is not necessary, for absorption features in reflectance are at the same wavelengths as in absorbance (with some qualifications due to scattering effects), and the same unique identifications can be made.

[1]Now at U.S. Geological Survey, Branch of Geophysics, Denver

Paper number 4B0270.
0148-0227/84/004B-0270$05.00

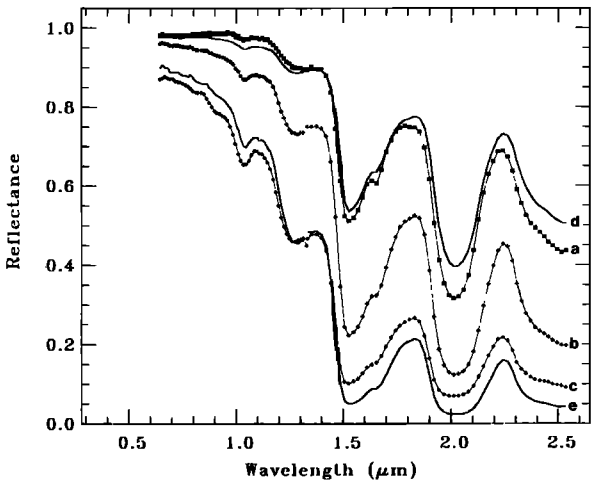

Fig. 1. The absolute bidirectional reflectance spectra of three different sizes of H_2O frost (data points) derived from *Clark* [1981*a*]. Curve a; fine-grained frost; b; medium-grained frost; and c; coarse-grained frost. Curve d is the K-M theory prediction of the fine grain size frost spectrum from the medium grain size data. Curve e is the K-M prediction of the coarse grain size frost spectrum from the medium grain size data.

However, in reflectance, the scattering of light in the particulate surface complicates the determination of mineral abundance. All remotely sensed identifications of minerals on the surfaces of the planets and satellites in the solar system have been done using spectral data in reflectance, not absorbance. The use of a scattering theory is then not primarily for mineral identification but to quantify the scattering problem so that mineral abundance and the microstructure of the surface might be derived.

New analysis techniques are a natural progression for understanding remotely sensed spectra of planetary surfaces, and several recent studies have introduced new methods, such as fitting Gaussians to absorption features in reflectance spectra [e.g., *Farr et al.*, 1980; *Clark*, 1981*a*; *Singer*, 1981; *McCord et al.*, 1981]. New studies have discussed the methods for particular cases but have not addressed the more general problem of the implications of the techniques in terms of understanding the general scattering problem in remote sensing studies. *Morris et al.* [1982] and *Mendell and Morris* [1982] have approached the problem from the use of Kubelka-Munk (K-M) theory, and suggested that the analysis of reflectance spectra should be performed using the K-M remission function versus photon energy. *Hapke* [1981] and *Hapke and Wells* [1981] presented an extensive discussion of the theory and application of reflectance spectroscopy. *Lumme and Bowell* [1981] and *Goguen* [1981] have presented theories similar to that of Hapke. Presented here is a discussion of the various methods in use and those proposed as they relate to practical analysis of reflectance spectra for use in planetary surface remote sensing studies.

KUBELKA-MUNK THEORY

The Kubelka-Munk (K-M) theory of diffuse reflectance has been discussed extensively by *Wendlandt and Hecht* [1966] and *Kortum* [1969]. It is not our intention to derive the equations from first principles but only to present the basic equation and discuss its implications and limitations. *Wendlandt and Hecht* [1966] and *Kortum* [1969] discussed extensively the limitations of the theory in general but did not discuss the limitations for geologic remote sensing.

The basic equation from K-M theory relates the remission function $f(r_\infty)$ to the diffuse reflectance from an infinitely thick medium of isotropic scatterers and is expressed as

$$f(r_\infty) = \frac{(1 - r_\infty)^2}{2r_\infty} = \frac{K}{S} \tag{1}$$

where r_∞ is the diffuse reflectance, K is an absorption coefficient, and S is a scattering coefficient. *Hapke* [1981] has shown that K and S are both related to Fresnel surface scattering and the volume absorption coefficient k and are inherently inseparable. The main limitations of K-M theory are that (1) it does not consider first-order Fresnel reflections; (2) it assumes isotropic scattering; and (3) mutual shadowing of particles is ignored. Also, for K-M theory to be strictly valid, the bihemispherical reflectance must be measured. This quantity is never measured in remote sensing but can be achieved, theoretically, under proper viewing geometry for isotropic scatterers. *Wendlandt and Hecht* [1966] and *Kortum* [1969] showed that as absorption increases, $f(r_\infty)$ shows a marked deviation from the linear trend ($f(r_\infty)$ proportional to absorption coefficient) predicted by K-M theory. Using *Wendlandt and Hecht*'s [1966] Figure III-11, $f(r_\infty)$ departs from linearity for values greater than about 0.1, corresponding to r_∞ less than about 0.64. Below this value of reflectance, the theory departs from observation. Both *Wendlandt and Hecht* [1966] and *Kortum* [1969] attribute this to the result of increased Fresnel reflection relative to the diffuse (higher order) reflection emanating from the surface. *Wendlandt and Hecht* [1966] and *Kortum* [1969] discussed methods which can be used to extend the theory to reflectances as low as 0.1, such as mixing the particles under study with a high-reflectance (white) material (such as colorless ground glass or some of the reflectance standard) to increase the multiple scattering. This is not practical in remote sensing and in any event can lead to band broadening, disappearance of vibrational structure, band shifts, and new bands [see *Wendlandt and Hecht*, 1966, and references therein].

An additional problem is that the quantity S is not easily derived and in practice is not separable from K. *Wendlandt and Hecht* [1966], show that wavelength dependent scattering can take the form λ^{-n}, where λ is wavelength and n is a constant between 0 and 4 when K-M remission is a function of energy. The K-M scattering parameter S, as a function of λ [see *Wendlandt and Hecht*, 1966, Figure III-8], has the form of

$$S = a + b\lambda^{-n} \tag{2}$$

where a and b are constant and a tends to increase as n increases. The parameter n tends to increase as the grain size approaches and becomes smaller than λ. Thus, in the range of validity of K-M theory ($r_\infty \geq 0.6$), the observation of reflectance increasing toward shorter wavelengths should be subtle. *Hapke* [1981] pointed out that small, submicron particles will be highly cohesive, and will tend to stick to the surfaces of larger particles or clump together into larger aggregates which would effectively appear as large particles with strong internal scattering. Thus, n will remain small. Two examples of wavelength dependent scattering are seen in the work by *Clark* [1981*b*, 1983]. *Clark* [1981*b*] shows a spectrum of a thin layer

of very fine grained frost (≤ 1−μm grain size) which shows reflectance decreasing linearly with wavelength. *Clark* [1983] shows a more interesting case where carbon black (grain size ~ 0.17 μm) is mixed with montmorillonite (grain size ~15 μm). Spectra of the pure end-members both show a decreasing reflectance toward shorter wavelengths. However, in mixture spectra, most notably when the carbon fraction is ~2 wt %, there is a significant increase in reflectance toward shorter wavelength (these spectra are also discussed later, in the section on continua, and the spectra are shown in Figure 5). In this case, the carbon particles are well separated [see *Clark* 1983] and appear more like a cloud of carbon particles (since the single scattering albedo of the montmorillonite is large), and diffraction becomes more important resulting in some Rayleigh scattering. In most cases, λ^{-n} scattering in surfaces is a very small effect compared to absorption in geologic material.

As an example of the problems which can be encountered when applying K-M theory, consider the spectra for three different grain sizes of H_2O frost shown in Figure 1 (curves a, b, and c). Reflectance spectra of different grain sizes can be computed from the remission function since S has been shown to be approximately in inverse proportion to grain size [see *Wendlandt and Hecht,* 1966, and references therein]. If we convert each spectrum to remission as shown in Figure 2*a* and divide the fine- and coarse-grained remission data by that for the medium-grained frost, the results should be constants describing the ratio of the grain sizes. However, we see in Figure 2*b* that ratios of the remission data are not constants. If we compute the mean value for each of the remission data ratios and then scale the remission data for the medium grained frost by these values, the fine- and coarse-grained frost spectra can be calculated by using the scaled remission data. However, when we do this we obtain curves d and e in Figure 1, which show considerable difference from the measured data. It should be pointed out that K-M theory does yield qualitative information. This can be seen by considering the predicted spectra mentioned above. It is obvious that both predicted spectra can be identified as solid H_2O based on the position of the absorption features. However, features such as band depths and widths differ from actual observations, thus making quantitative analysis of these features error prone (see the section on absorption features modeled as Gaussians for an example using this data).

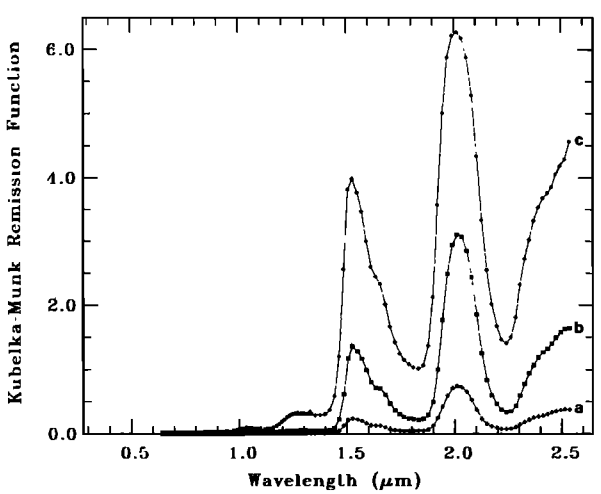

Fig. 2*a*. The K-M remission function of the three H_2O frost spectra (curves a, b, and c) in Figure 1: fine grains for curve a, medium grains for curve b, and coarse grains for curve c.

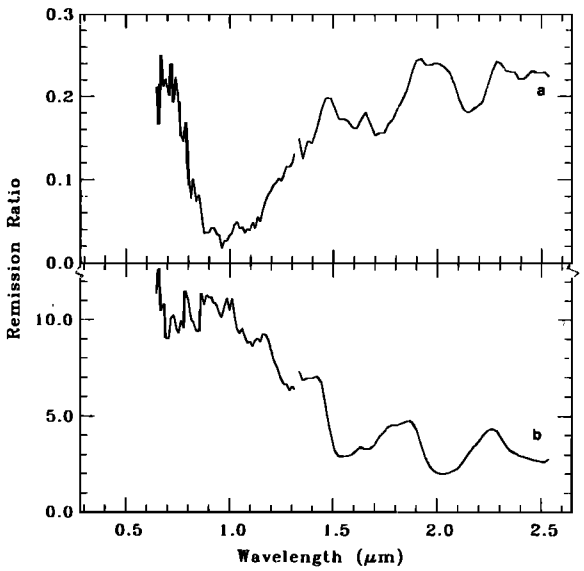

Fig. 2*b*. The ratio of the remission data for the fine- and coarse-grained frost to the medium-grained frost. Curve a is fine/medium, and curve b is coarse/medium. The calculated mean value of the ratio is about 0.148 for curve a, 6.62 for curve b, and a peak to peak variation of about a facter of 5–10. This variation results from the difference in the mean optical path length of photons inside and outside an absorption feature, thus also varying the scattering.

The ratio of the remission spectra of the same material of two different grain sizes should appear like a constant or a constant plus a λ^{-n} term as in equation (2). The mean values of the remission ratios of Figure 2*b* were calculated to be 6.62 and 0.148 for the coarse- and fine-grained ratios of the remittance data of frost relative to the medium-grained frost, respectively. However, as seen in Figure 2*b*, the remission ratios show significant variation. This shows that in a particulate surface such as solid H_2O, the scattering changes with absorption coefficient. Photons will be scattered less in an absorption band, because of increased absorption, than outside the band. The mean path length that photons travel in the material is wavelength dependent, and an absorption band will always be weaker than predicted by the absorption spectrum and constant scattering parameter. In other words, the absorption feature will always appear slightly saturated. The applicability of K-M theory is that it converts reflectance over a limited range into a quantity proportional to the absorption coefficient of the material.

BIDIRECTIONAL REFLECTANCE THEORIES

Several recent papers [*Hapke,* 1981; *Goguen,* 1981; *Lumme and Bowell,* 1981] present extensive discussions concerning the role of scattering as it relates to reflectance spectroscopy. The applicability of these theories is that they model the realistic interaction of electromagnetic radiation with a particulate surface and as such can yield information about surface microstructure as well as individual mineral abundances. All authors use basic radiative transfer equations to derive scattering theories which deal with particulate surfaces. Although these theories differ in specific detail, all include variables and expressions for specular and diffuse reflectance, phase depen-

dent particle scattering, and mutual interparticle shadowing. The parameters in these theories are directly related to physical properties of the surface such as the density of particles in the surface, roughness of the surface viewed by the detector, grain size, and the complex index of refraction of the material. As an example of one of these scattering equations, consider equation (16) of *Hapke* [1981]:

$$r(\bar{w},\lambda,\mu_o,\mu,g) = \frac{\bar{w}}{4\pi}\frac{\mu_o}{\mu_o+\mu}\left\{[1+B(g)]P(g) + H(\mu_o)H(\mu) - 1\right\} \quad (3)$$

where r is the reflectance at wavelength λ, μ_o is the cosine of the angle of incident light, μ is the cosine of the angle of emitted light, g is the phase angle, $\bar{w}$ is the average single scattering albedo, $B(g)$ is a backscatter function, $P(g)$ is the average single particle phase function, and H is the *Chandrasekhar* [1960] H function for isotropic scatterers. This function seems to work well for dark surfaces, but when $r > 0.9$, Hapke's approximation of the H functions shows considerable error and equation (3) shows deviation from measurements. The expressions developed by *Lumme and Bowell* [1981] and *Goguen* [1981] are similar, and it may turn out that some combination of these theories would result in a generally acceptable expression. Laboratory studies [*Hapke and Wells,* 1981; *Goguen,* 1981] and analysis of planetary data [*Lumme and Irvine,* 1982] using the various theories show encouraging results.

The single scattering albedo, a variable common to all these theories, is the probability that a photon survives an interaction with a single particle and as such includes Fresnel reflection, absorption, scattering, and diffraction due to the presence of an individual grain. *Hapke* [1981] developed the theory further by deriving a relationship between the single scattering albedo, the complex index of refraction, the grain size, and a scattering parameter to describe scattering centers within nonperfect grains. The single scattering albedo of a grain can be found from his equation (24):

$$w = S_l + \frac{(1-S_l)(1-S_l)\left\{r_1 + \exp\left[-2(k(k+s))^{1/2}D/3\right]\right\}}{1 - r_1 S_l + (r_1 - S_l)\exp\left[-2(k(k+s))^{1/2}D/3\right]} \quad (4)$$

where S_l and S_l can be computed from the complex index of refraction [see *Hapke,* 1981, equation (21)] and are the external and internal scattering coefficients, respectively, s is a scattering coefficient, D is the particle diameter, k is the absorption coefficient (note Hapke uses α instead of k here), and

$$r_1 = \frac{1 - [k/(k+s)]^{1/2}}{1 + [k/(k+s)]^{1/2}} \quad (5)$$

The importance of equation (4) can be illustrated by considering that w can be derived by reflectance measurements over a variety of phase angles. In a monomineralic surface, $w = \bar{w}$. For a multimineralic surface, $\bar{w}$ can be computed from equation (17) of *Hapke* [1981]. This is further discussed below in the quantitative analysis section. Assuming that the number and types of minerals can be identified solely by their characteristic absorption features, equation (4) has the potential for determining individual mineral abundance and grain size. Thus, from a geologic perspective, knowing the types, abundance, and size distribution of minerals allows us to address what geologic processes have been active on the surface.

REFLECTANCE TYPES

Reflectance spectra for applications to remote sensing problems are typically measured in one of the three following forms: directional-hemispherical reflectance (A_H, equation (40) of *Hapke* [1981], bidirectional reflectance (r_i, formally called the bidirectional radiance coefficient by *Hapke* [1981, equation (37)]), and the geometric albedo (p, equation (44) of *Hapke* [1981]). The reader is referred to *Hapke* [1981] for derivation of the equations. None of the above mentioned forms of reflectance are always equal to true diffuse reflectance r_∞ (or bihemispherical reflectance r_o, as defined by *Hapke* [1981, equation (34)]) but are sometimes conditionally equal to it.

The directional-hemispherical reflectance is the ratio of power emitted from a surface in all directions to the irradiance of a collimated light source incident from a specific direction. A surface of isotropic scatters illuminated at an incidence angle i of 60° will have the directional-hemispherical reflectance equal to the bihemispherical reflectance [e.g., *Hapke,* 1981]. However, the angle of incidence i or emission e of commercial spectrometers that use an integrating sphere is typically 0° [e.g., *Adams,* 1975].

The bidirectional radiance coefficient (nearly always called bidirectional reflectance) is the brightness of a surface relative to the brightness of a Lambert surface identically illuminated. Most remote sensing data of small areas of a planetary surface are of this type: the sun illuminates the surface with an angle of incidence i from the surface normal and the surface is viewed (e.g., from a spacecraft or telescope) at the angle of emission e, and phase angle g between the sun, surface, and viewer. All the work done at the Planetary Geosciences Division, University of Hawaii laboratory is of this type [e.g., *Clark,* 1981*a, b,* 1983; *Singer,* 1981]. Other studies that measured bidirectional reflectance are those by Hunt and colleagues [see *Hunt and Salisbury,* 1976, and references therein] and *Pieters* [1983].

Hapke [1981] showed that the bidirectional radiance coefficient is formally equal to the bihemispherical reflectance for a surface of isotropic scattering particles when $i = e = 60°$ and g is large enough that the opposition effect is negligible ($B(g) \cong 0$).

The geometric albedo is the ratio of the brightness of the integral hemispherical disk of a planet to the brightness of a flat Lambert disk viewed normally at zero phase. In the case of isotropic scatterers and ignoring the opposition effect,

$$p \cong \frac{r_\infty}{2} + \frac{r_\infty^2}{6} \quad (6)$$

where p is the geometric albedo [*Hapke,* 1981]. Other authors have derived equally simple equations relating a reflectance to geometric albedo [e.g., *Veverka et al.,* 1978].

The determination of the correct reflectance level of a remotely obtained spectrum is often difficult. A reflectance standard is usually not available on the surface, especially for data obtained from aircraft, spacecraft, or of other planets through telescopes. Thus, the reflectance level is derived from the flux levels received by the instrument, a knowledge of the area viewed, and the incident solar flux. Sometimes in astronomy (a small asteroid, for example), the size of the area viewed is not known because the object is a point source in the

telescope, and the object size is poorly known, if at all. The reflectance level is often in error by a multiplicative factor of 10% or more due to these calibration problems [e.g., see *Veverka*, 1977]. This uncertainty further invalidates the use of K-M theory because of the nonlinear nature of the remission function. This calibration difficulty has led to a common practice of scaling the remotely sensed reflectance spectrum to unity at some wavelength.

MEAN OPTICAL PATH LENGTH

The distance x that a photon travels in a material with absorption coefficient k is related to the probability that the photon will not be absorbed. In other words, light is attenuated according to Beers law:

$$I = I_0 e^{-kx} \tag{7}$$

where I_0 is the initial intensity and I is the attenuated intensity. When a boundary is encountered where there is a change in the index of refraction, the light will be reflected and refracted. Thus, all photons do not travel the exact same path after encountering a boundary.

As an example, consider a plane parallel slab with a thickness d and an index of refraction n in a vacuum with parallel light normally incident on the slab face. At the two boundaries, the light reflected, C_R, is given by Fresnel's formulas [see *Wendlandt and Hecht*, 1966]. It can be shown that the transmitted light is

$$I(k) = (1 - C_R)^2 I_0 \left[\sum_{i=0}^{\infty} C_R^{2i} e^{-(2i+1)kd}\right]$$

$$= I_0 \frac{(1 - C_R)^2 e^{-kd}}{1 - C_R^2 e^{-2kd}} \tag{8}$$

Since some light is reflected at each boundary, some light travels a distance d, $3d$, $5d$, or more. Thus the average distance traveled by photons in the medium is greater than d. We define this average distance to be the mean optical path length (mopl). If we define $\bar{d}$ to be the mean optical path in the slab, then the light absorbed is

$$1 - e^{-k\bar{d}} \equiv \left[I(k = 0) - I(k)\right] / I(k = 0) \tag{9}$$

Solving for the mean optical path length from equations (8) and (9), we find

$$\bar{d} = \frac{-1}{k} \ln \left[\frac{(1 - C_R^2) e^{-kd}}{1 - C_R^2 e^{-kd}}\right] \tag{10}$$

For a material such as common glass with $C_R = 0.04$ and k very small, $\bar{d} = 1.0032d$.

In a particulate surface, the light usually encounters many index of refraction boundaries so that tracing the photon paths is quite complex. Since scattering in the surface only redirects photons and it is the passage through the various materials that cause the absorption, there is a mean path length $\bar{l}$ which can be used to describe the absorption process

$$r \equiv e^{-k\bar{l}} \tag{11}$$

where r is any type of reflectance of the surface scaled to unity in the case of no absorption (e.g., nonisotropic scattering and no absorption could result in nonunity bidirectional reflectance). Equation (11) implies that one can easily obtain the absorption coefficient with simple mathematical manipulation if the path length is known. The "apparent absorbance" [*Kortum*, 1969] is

$$A_p = -\ln (r) \tag{12}$$

and implies that with equation (11), A_p is proportional to the absorption coefficient k. However, this is not exactly the case, since the mopl can vary considerably and depends on k [e.g., see *Pieters*, 1983].

An expression for the mean optical path in a particulate surface can be derived using the reflectance theory of *Hapke* [1981]. Using equations (3) and (11)

$$\bar{l} = \frac{1}{k} \ln \left[r(\bar{w}, \lambda, \mu_0, \mu, g) / r(\bar{w} = 1.0, \lambda, \mu_0, \mu, g)\right] \tag{13}$$

Using the approximation of *Hapke* [1981] for the H function,

$$H(\bar{w}, \mu) = \frac{1 + 2\mu}{1 + 2\sqrt{(1 - \bar{w})}} \tag{14}$$

equation (13) becomes for an isotropic case, $P(g) = 1.0$, and letting $B(g) = 0.0$,

$$\bar{l} = \frac{-1}{k} \left\{\ln \bar{w} - \ln \left[1 + 2\mu \sqrt{(1 - \bar{w})}\right] - \ln \left[1 + 2\mu_0 \sqrt{(1 - \bar{w})}\right]\right\} \tag{15}$$

The single scattering albedo $\bar{w}$ can be computed using equation (4) but *Hapke* [1981] showed equation (4) can be approximated by

$$\bar{w} = (1 + 2kD)^{-1} \tag{16}$$

Using the approximation $\ln(1 + x) = x$, when kD is small, and substituting equation (16) for $\bar{w}$, equation (15) becomes

$$\bar{l} = 2D + \frac{2(\mu + \mu_0)\sqrt{2D}}{\sqrt{k(1 + 2kD)}} \tag{17}$$

Hapke [1981] has shown that equation (16) is valid over the same range as K-M theory. Since kD is usually small (Hapke cites a reflectance of ~0.06 when $kD = 1.5$, the $\sqrt{1 + 2kD}$ term is nearly constant. Then, when the grains are optically thin ($k < D$ and $kD < 1$), $\bar{l}$ is essentially inversely proportional to the square root of the absorption coefficient.

The mean optical path in a single grain is

$$\bar{l}' = \frac{-1}{k} \ln(\bar{w}) \tag{18}$$

since the single scattering albedo represents all the light that encounters a particle and is not absorbed. The mean number of particles encountered by photons in the surface is given by

$$m = \frac{\ln r}{\ln \bar{w}} \tag{19}$$

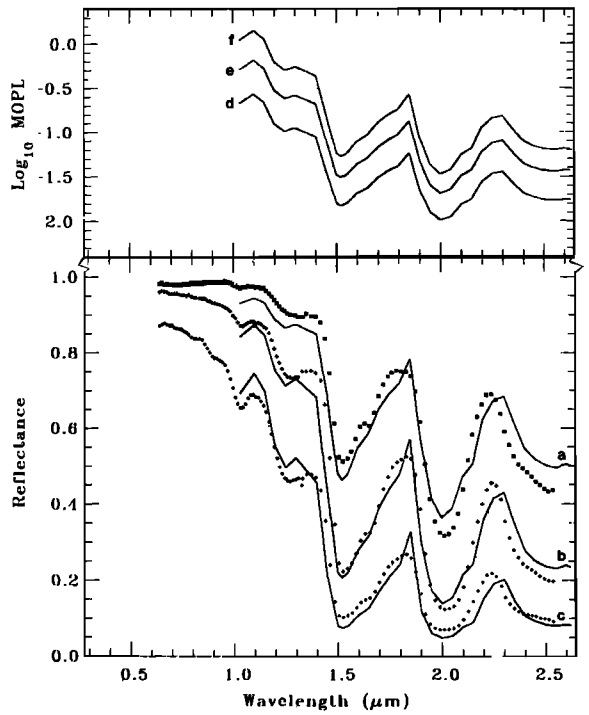

Fig. 3*a*. Laboratory spectra of water ice of three different grain sizes (points) in the near infrared from *Clark* [1981*a*] are compared to theoretical computations (lines) using the complex index of refraction for water ice [*Irvine and Pollack*, 1968] and equations (15), (16), (22), and (23). Reasonable matches of theoretical spectra were for grain sizes of 5 μm (curve a), 30 μm (curve b), and 150 μm (curve c). The general agreement is encouraging; however, some differences are noted in the text as probably being due to errors in the ice absorption coefficients. At the top of the figure is the mean optical path length as a function of wavelength for each grain size, curve d is 5 μm, curve e is 30 μm, and curve f is 150 μm. It is seen that the more the material absorbs light, the less the photons travel in the particulate surface. The log mean optical path spectrum mimics the reflectance spectrum.

The mopl of a particulate surface can also be expressed as

$$\bar{l} = m\bar{l}' \tag{20}$$

In the case where the grain is optically thin, it can be shown, using equations (16) and (18), that

$$\bar{l}' \cong 2D \tag{21}$$

then the mopl, $\bar{l}$, is $2mD$. Since the mopl is approximately inversely proportional to the true absorbance (or absorption coefficient), we see from equations (11) and (12) that the apparent absorbance is approximately proportional to the square root of the absorption coefficient.

Equation (11) is the reflectance relative to the reflectance of a surface with the same scattering conditions but no absorption. However, this equation does not include first-order Fresnel reflection from crystal surfaces. This can be simplistically modeled by the equation

$$r = (e^{-k\bar{l}} + s_i) / (1.0 + s_i) \tag{22}$$

where s_i is the first-order Fresnel reflection, which in the bidirectional reflectance case at low phase angles is

$$s_i = \frac{(n-1)^2 + (\frac{k\lambda}{4\pi})^2}{(n+1)^2 + (\frac{k\lambda}{4\pi})^2} \tag{23}$$

where n is the real part of the index of refraction and k is the absorption coefficient.

An example computation, using the above theory is illustrated by using the complex index of refraction data for water ice from *Irvine and Pollack* [1968], and equations (15), (16), (22), and (23). Results are shown in Figure 3*a* compared with laboratory data. The agreement is reasonable except for a couple of areas which appear to be due to errors in the absorption coefficient data. For example, the peak at 1.85 μm appears inconsistent with both diffuse reflectance spectra [e.g., *Clark*, 1981*a*] and transmission spectra of ice [e.g., *Ockman*, 1957]. Similarly, the step in the 2-μm absorption feature near 2.1 μm also is inconsistent since the absorption appears symmetric in laboratory spectra. The photon mean optical path for each grain size for this spectral region is shown in Figure 3*a* top, and the decrease in the path in an absorption feature is nicely illustrated.

Using the measured reflectance of the medium-grained frost, a grain size of 30 μm, and index of refraction data from *Irvine and Pollack* [1968], the absorption coefficient was determined by an iterative process using equations (15), (16), (22), and (23). The derived absorption coefficient is compared to the *Irvine and Pollack* [1968] absorption coefficient for solid H_2O in Figure 3*b*. In order to compare the spectra predicted by both K-M and the method outlined above, the derived absorption coefficient of the medium-grained frost was used to calculate the reflectance spectrum of the fine- and coarse-grained frost using the grain sizes determined for Figure 3*a*. The calculated spectra are compared to measured data in Figure 3*c*. The predicted spectra were divided by the measured data, and these ratios are plotted in Figure 3*d*. Both plots illustrate that the scattering theory approach outlined above result in better prediction of measured reflectance than K-M theory. However, in regions of strong absorption the scattering theory predictions also show variations from measured data. This difference is at least partly due to the

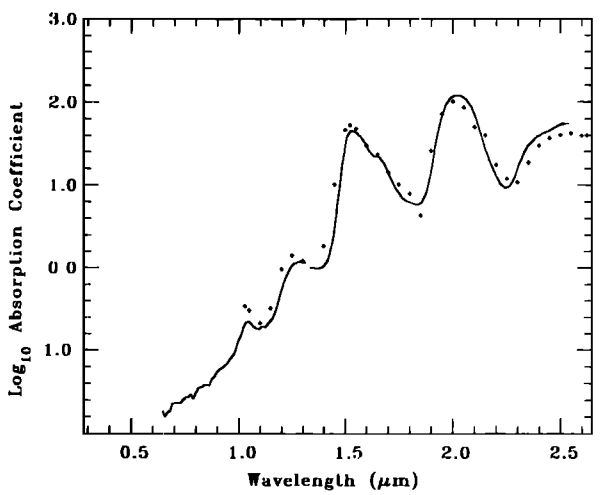

Fig. 3*b*. *Irvine and Pollack* [1968] water ice absorption coefficient data (points) and derived absorption coefficient of the 30 μm grain sized frost (line) are compared.

approximation of equation (16) and can be reduced by using equation (4) to determine w (the quantitative analysis section further explores this point).

The photon mean optical path should not be confused with the mean penetrated layer thickness (mplt). The mopl is the mean distance traveled in a random walk, while the mplt is a perpendicular linear distance from the surface that photons penetrate and is considerably less than the mopl. The mplt is also dependent on the single scattering albedo of the grains. If we consider the scattering to be isotropic and the distance between grains is d_0, then a photon will be scattered, on the average, a distance $(\pi/4)d_0$ in the upward or downward direction in the surface. The mean distance that photons penetrate into the surface is easily computed from a one-dimensional random walk problem. If, on the average, photons are scattered m times before leaving the surface (see equation (19)), then it takes $m/2$ scatterings to reach the mplt point, and the thickness penetrated, t_m, is

$$t_m = \frac{\pi}{4} d_0 \sqrt{\frac{m}{2}} \tag{24}$$

Note that this thickness is the $1/e$ depth and that an optically thick layer should be several times this thick.

Absorption Features Modeled as Gaussians

Since absorption features are usually considered to be Gaussian-like when analyzed as absorption coefficient versus photon energy [e.g., *Smith and Strens,* 1976], we need to know the implications for spectral analysis in apparent absorbance. An absorption can be modeled with a Gaussian of the form

$$G(\vartheta, w, G_0, \vartheta_0) \equiv G_0 \exp\left[-\ln 2\left(\frac{\vartheta - \vartheta_0}{W}\right)^2\right] \tag{25}$$

where G_0 is the intensity of the Gaussian, W is the full width at half maximum (in frequency units), ϑ_0 is the center frequency, and ϑ is the frequency of light.

Since the apparent absorbance is approximately proportional to the square root of the absorption coefficient, then the apparent absorbance is approximately proportional to the square root of the Gaussian:

$$A_p \propto G_0^{1/2} \exp\left[-\ln 2\left(\frac{\vartheta - \vartheta_0}{\sqrt{2}\,W}\right)^2\right] \tag{26}$$

Thus, Gaussians in true absorbance are also Gaussians in apparent absorbance when the grains are optically thin ($k < D$ and $kD < 1$) except that the Gaussians in apparent absorbance have a smaller intensity and a width which is a factor of $\sqrt{2}$ larger. Note that in a multimineralic surface, only the mineral grains causing the absorption feature need to be optically thin.

This relationship is also demonstrated with K-M theory. The remission function $f(r_\infty)$ is proportional to the absorption coefficient. Thus by combining equations (1) and (25) we see

$$G_0 \exp\left[-\ln 2\left(\frac{\vartheta - \vartheta_0}{W}\right)^2\right] \propto \frac{(1 - r_\infty^2)}{2r_\infty} \tag{27}$$

From equations (26), (27), and (12), a Gaussian description of an absorption feature using K-M theory would predict that

$$\frac{(1 - r_\infty^2)}{2r_\infty} \propto \frac{1}{2}\left[\ln(r)\right]^2 \tag{28}$$

It is easily shown that the two sides of equation (28) agree to better than 2% of each other within the validity of K-M theory (i.e., $r_\infty > 0.6$), and the difference corresponds to only a 0.5% error when converted to reflectance, well within the error of most reflectance measurements. The relationship presented in equation (28) is illustrated by Figures 4*b*–4*e*, which were computed from the hematite reflectance spectrum in Figure 4*a*. Noting $A_p = -\ln(r)$ and comparing equation (27) with (28), we see that the Gaussian amplitude of K-M theory is one half the square of that in apparent absorbance and the Gaussian width is $\sqrt{2}$ smaller in K-M theory (as $r \to 1$).

As discussed earlier, there is often a 5–10% error (or more)

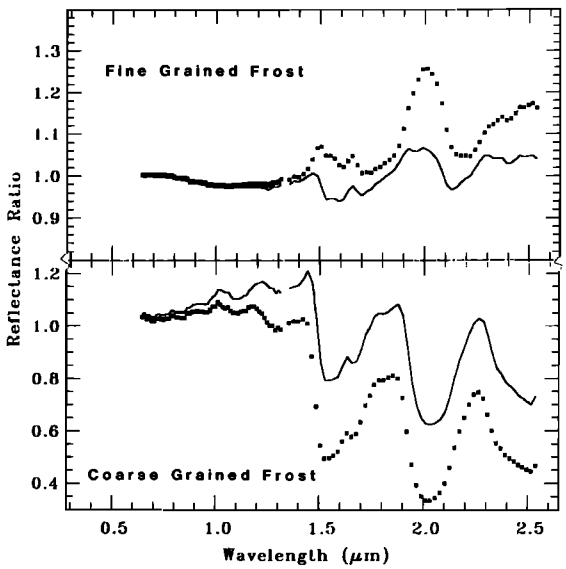

Fig. 3*d*. Ratio of predicted to measured reflectance of K-M (points) and methods presented in this paper (lines) for fine-grained frost (top) and coarse-grained frost (bottom) are compared. K-M is less accurate than the simplified *Hapke* [1981] theory.

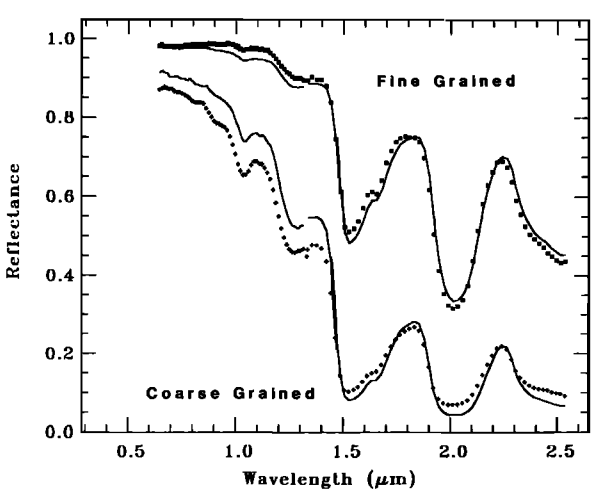

Fig. 3*c*. Laboratory reflectance data for fine and course grained H_2O frost (points) are compared with the predicted reflectance using derived absorption coefficient of the medium frost and equations (15), (16), (22), and (23) (lines).

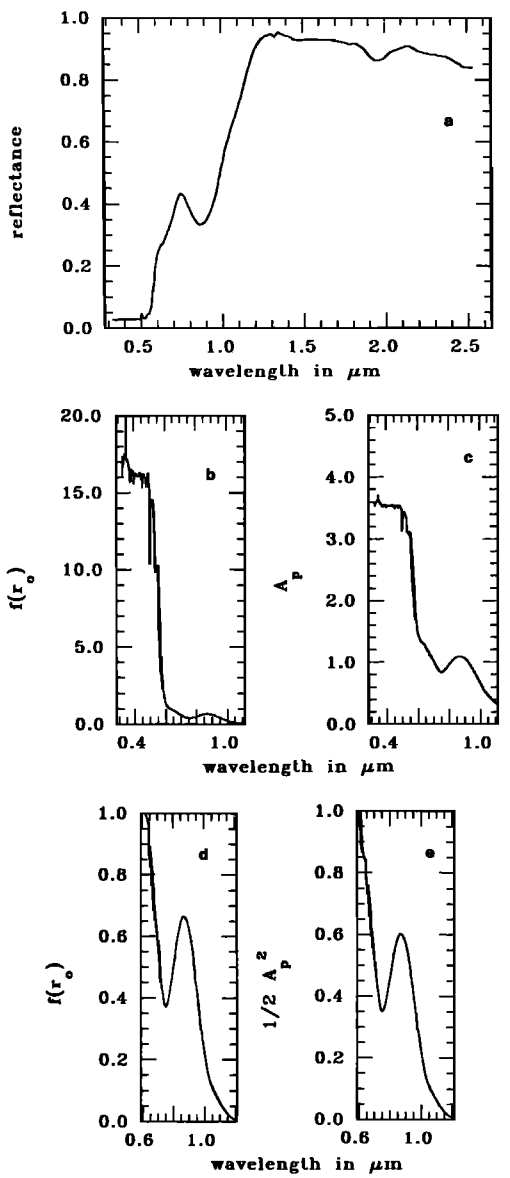

Fig. 4. (*a*) The reflectance spectrum of hematite from *Singer* [1982]. Note that the strong UV absorption does not approach zero below 0.5 μm. This is due to specular reflection. (*b*) The K-M remission of the hematite spectrum in Figure 4*a* is compared to (*c*) the apparent absorbance of the hematite spectrum. Both K-M remission and apparent absorbance suffer from the effects of band saturation caused by specular reflection and by differing mean optical path lengths in and out of absorption bands. The similarity of (*d*) the K-M remission function to (*e*) 1/2 the apparent absorbance squared is shown when the reflectance is high.

in deriving the reflectance level in remotely sensed spectra. This can lead to analysis problems when using K-M theory and a Gaussian absorption feature analysis. If there is a multiplicative error in r_∞ then the width W and the intensity G_0 of the Gaussian changes. However, in apparent absorbance, an error in the reflectance is equivalent to a Gaussian plus a constant, and there is no width or intensity change. For example, if the medium-grained frost spectrum in Figure 1 is multiplied by 0.9, the 1.04-μm band intensity in the remission function increases by a factor of 1.77, while the band width increases by a factor of 1.12 relative to the remission function of the unscaled spectrum.

Morris et al. [1982] and *Mendell and Morris* [1982] discussed the problem of band saturation in reflectance and noted that the fitting of Gaussians in reflectance could lead to spurious multiple Gaussians fitted to a saturated reflectance feature. *Morris et al.* [1982] incorrectly stated that Gaussian fitting to ln (r) would also yield spurious multiple Gaussians. The above discussion shows mathematically that Gaussians in K-M remission space are also Gaussians in apparent absorbance in the range of validity of K-M theory.

Fresnel reflection is the one major problem in analysis of reflectance spectra shared by both K-M theory and apparent absorbance. The reflectance observed from a surface is

$$r = r_1 + r_m \tag{29}$$

where r_1 is the fraction of reflected light from the first-order specular reflection component and r_m is the light which has entered one or more particles and is eventually scattered out of the surface. At small phase angles, r_1 and s_f from equation (23) are equal. Since r_1 cannot be separated from r_m in most cases, both apparent absorbance and K-M theory can suffer from band saturation. This is seen in Figure 4*a* for the case of hematite where there is obvious band saturation shortward of 0.5 μm in the reflectance spectrum which also appears in remission (Figure 4*b*) and apparent absorbance (Figure 4*c*). Since the UV absorption in the hematite is saturated even in remission, it is not practical to fit Gaussians to the feature such that the wing of the Gaussian defines the continuum of the 0.86-μm absorption feature as proposed mathematically by *Mendell and Morris* [1982]. The band saturation would cause problems in defining a unique Gaussian which realistically described the absorption feature. In practice, other smooth curves, such as a polynomial, would be indistinguishable from a Gaussian over the narrow wavelength range.

Clark [1981*a*] fit Gaussians to water frost spectra of various grain sizes with a size range of over 10. As the 2.02-μm absorption increased, the band saturation effect became obvious in reflectance. However, the analysis was performed using ln (r) versus energy, and no additional Gaussians were needed to characterize the feature as the band grew. Band saturation could have become a problem if stronger bands were analyzed.

THE CONTINUUM PROBLEM

An apparent continuum is a mathematical function used to isolate a particular absorption feature for analysis of a spectrum [e.g., see *Clark*, 1981, 1983; *McCord et al.*, 1981; *Singer*, 1981]. As such, it represents the absorption due to a different process in a specific mineral or possibly absorption from a different mineral in a multimineralic surface.

An example of continuum use is shown in Figure 5 with montmorillonite-carbon black mixtures. Montmorillonite has absorption features due to chemically and physically absorbed H_2O at 2.8, 2.2, 1.9, and 1.4 μm and other absorptions such as a charge transfer whose wing extends from the visible to past 1 μm. If only the 1.4-, 1.9-, and 2.2-μm absorptions are to be analyzed, then the effects of the other features must be removed from the analysis. This is typically done by estimating the absorptions from the other processes by a suitable function (straight-line segments, polynomial, a Gaussian, etc.). The continua shown in Figure 5 are cubic splines, although straight-line segments would produce nearly the same result in this case.

The continua can be modeled using the mean optical path length through different materials or separated into different absorption processes using the equation

$$e^{-(\bar{k}\,\bar{l})} \equiv \exp\left[-\sum_{i=1}^{i} k_i \bar{l}_i\right] \tag{30}$$

where $\bar{k}$ and $\bar{l}$ are the equivalent absorption coefficient and mopl, respectively, for the surface as a whole, k_i is the absorption coefficient of the ith material having a mopl $\bar{l}_i$ for a multimineralic surface in an intimate mixture. Also, k_i may represent the absorption coefficient for a particular absorption process and having a particular mopl, $\bar{l}_i$. Thus, the removal of a continuum for a particular spectrum should be done as a division if the spectrum is in reflectance or as a subtraction in apparent absorbance (many examples of continuum removal can be found in the references in the first paragraph of this section).

The continuum removal for the montmorillonite plus carbon black mixtures can be expressed as

$$r(\lambda) = e^{(-k_1\bar{l}_1)}e^{(-k_2\bar{l}_2)}e^{(-k_3\bar{l}_3)} \tag{31}$$

where the k_i and $\bar{l}_i$ are a function of wavelength λ. If $k_1\bar{l}_1$ represents the absorption (in terms of optical depth) due to the adsorbed H_2O in the montmorillonite, $k_2\bar{l}_2$ the absorption due to other processes in the montmorillonite, and $k_3\bar{l}_3$ represents the absorption due to the carbon black, then to remove the absorption effects of all but those for H_2O, a continuum representing $e^{(-k_2\bar{l}_2)}e^{(-k_3\bar{l}_3)}$ must be ratioed with the reflectance spectrum, or subtracted from the apparent absorbance spectrum. The resulting absorptions retain their original function. For example, if the absorption is a Gaussian in the apparent absorbance presentation, it is still a Gaussian in a continuum removed presentation (if $k_i < D_i$ and $k_iD_i < 1$). Removal of a continuum by dividing it into the reflectance spectrum is not valid for analysis in K-M remission since after continuum removal, the data are no longer bihemispherical reflectance. Continuum removal by subtraction from K-M remission data is valid, however.

There is another important reason for the use of a continuum in analysis of reflectance spectra. There may be wavelength dependent scattering which imparts a slope to the spectrum (discussed by *Wendlandt and Hecht* [1966] and *Morris et al.* [1982]) which causes apparent shifts in the band minimum. Also, in multimineralic surfaces, one component may impart a significant slope to the spectrum (e.g., lunar soils [see *McCord et al.*, 1981]). In the case of lunar soils, there are pyroxene absorptions at 1 and 2 μm superimposed on a very red slope (reflectance increasing toward longer wavelengths). Usually this red slope is so great and the pyroxene absorptions so weak that there exists no minima in the reflectance [e.g., see *McCord et al.*, 1981]. Clearly, a continuum must be used to analyze the absorption features. As the continuum slope increases, the apparent band minimum (not the true band center) will shift to shorter wavelengths for a red slope and to longer wavelengths for a blue slope. However, removal of the continuum slope will correct the band minimum to that of the true band center.

The definition of a continuum also provides a more consistent definition of band depth. The band depth D_B is defined as

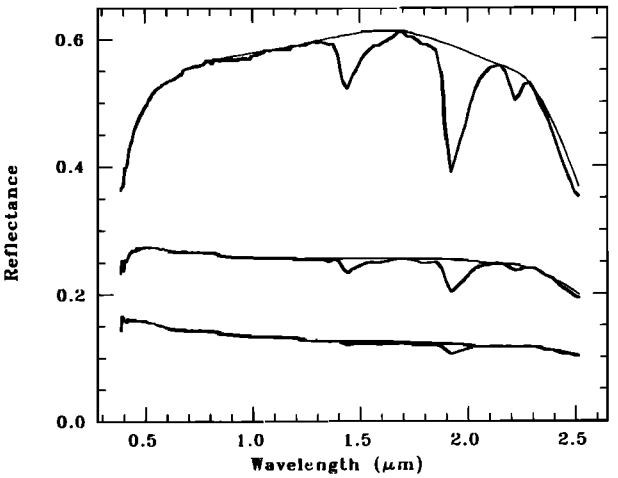

Fig. 5. The spectra of pure montmorillonite (top) and mixtures of montmorillonite plus carbon black (0.5 wt % carbon black, middle; 2.0 wt % carbon black, bottom) from *Clark* [1983] are shown with example continua for the purpose of analyzing the bound water absorptions in the montmorillonite. The continua represent the absorption due to all processes except of water in the montmorillonite. The continuum should be removed from the reflectance spectrum by division (reflectance/continuum) or subtracted from the apparent absorbance (−ln reflectance).

$$D_B \equiv \frac{R_C - R_B}{R_C} \tag{32}$$

where R_B is the reflectance at the band center and R_C is the reflectance of the continuum at the band center. *Morris et al.* [1982] presented an alternative definition of band depth (which we will label D_M) which is equal to the reflectance of the continuum minus the reflectance of the spectrum. If there is a multiplicative error in the reflectance level, there is a corresponding error in the band depth D_M. The band depth should imply the amount of light absorbed. Consider the hypothetical case where the general reflectance level is 20% (continuum = 0.2), but there exists a wavelength where all light is absorbed (reflectance = 0.0); then $D_B = 1.0$, but $D_M = 0.2$. In this case, D_M implies that 20% of the light due to the absorption feature is absorbed, whereas all the light has been absorbed. Clearly, D_B is a more realistic description of the situation. Examples of D_B applications can be found in the work by *Clark* [1981*a*, 1983].

A variation of the D_M band depth method has been applied to normalized spectra. For example, *Charette et al.* [1976] fit a continuum representative of iron absorption to laboratory spectra of lunar soils which had been scaled to unity at 0.56 μm. The continuum was then subtracted, and a Gaussian was fit to the remaining spectrum. Since the lunar soil spectra increase in reflectance at longer wavelengths, the continuum values at 1 μm ranged from about 1.3 to over 1.6. If all the light at 1 μm were absorbed, the band depths computed using D_M would be greater than 100%. In fact, if the continuum reflectance were 1.6 at the band center and the reflectance of the spectrum were 0.6, the D_M would be 100%, while D_B would be only 62.5%. Thus, any band depth value can be obtained by scaling the spectrum and using the D_M computation.

QUANTITATIVE ANALYSIS USING SCATTERING THEORY

The new scattering theories by *Hapke* [1981], *Lumme and Bowell* [1981], and *Goguen* [1981] provide the potential for

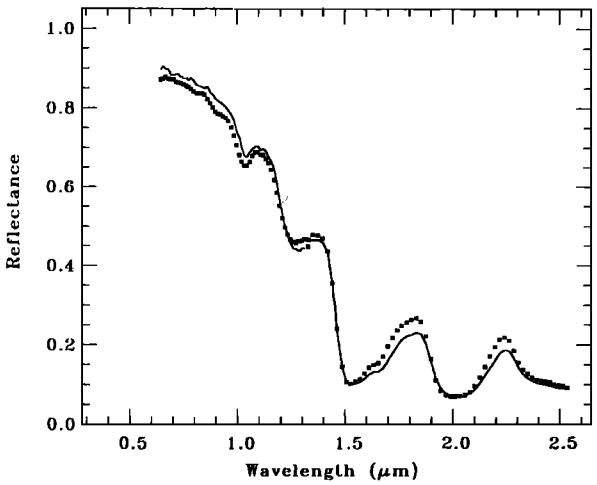

Fig. 6*a*. Laboratory reflectance spectrum of coarse-grained frost (points) is compared to a calculated reflectance spectrum (line) applying the full *Hapke* [1981] theory with ice grains of three different sizes as outlines in the text.

quantitative inversion of a reflectance spectrum of a multimineralic surface to actual mineral abundance. As stated earlier, most presentations of such theories are in terms of deriving absorption coefficient from laboratory reflectance data, given the grain size of the material present [e.g., *Hapke and Wells,* 1981]. From the above theories, one usually solves for the single scattering albedo, the single particle phase function, and a compaction parameter.

By observing the surface for different viewing conditions, $\bar{w}$ can be derived from basic reflectance equations, such as equation (3). From equation (17) of *Hapke* [1981], the average single scattering albedo of a homogeneous, multicomponent surface can be found at each wavelength from

$$\bar{w} = \left[\sum_i \frac{M_i}{\varrho_i D_i} w_i\right] \Big/ \left[\sum_i \frac{M_i}{\varrho_i D_i}\right] \tag{33}$$

where i refers to the ith component, M_i is the mass fraction, ϱ_i is the density of the material, D_i the mean grain diameter, and w_i the single scattering albedo of the ith component.

The single scattering albedo of a grain can be found from equation (4), and once it has been computed, there are six unknowns; k_i, n_i, s_i, D_i, M_i, and ϱ_i, per ith component in the surface at one wavelength. Only k is a strong function of wavelength. The index of refraction varies a small amount with wavelength, and s might tend to increase slightly toward shorter wavelengths. Assuming that n and s are constant and that there are z wavelengths and j components, we have z equations for the average single scattering albedo $\bar{w}$ and $[(z + 5)j)] - 1$ unknowns. If all these are actually unknown for a surface of only one component, then the best that one can hope to do is solve for the product kD assuming n, s, and ϱ.

As stated in the introduction, the materials are not identified from the absorption coefficient but from absorption features in the reflectance spectrum. If a material cannot be identified from its reflectance spectrum (e.g., no observable features), any conversion to absorbance will not produce additional features or increase the probability of identification. Thus, if the materials can be identified, then the densities and complex indices of refraction are known or can be measured with suitable samples. The problem is then reduced to z equations and $3j$ unknowns (s_i, D_i, and M_i). The mass fractions M_i of the individual components can be solved for using a nonlinear least squares technique.

In reality, particulate surfaces of even one material consist of a range of grain sizes. Such a case can be modeled using equations (4) and (33) where each component is the same material but of varying grain sizes. As an example of this application, three grain sizes (20, 100, and 1000 μm with weight fractions of 2, 8, and 90%, repectively) were used to predict the coarse-grained frost reflectance spectra with the full *Hapke* [1981] theory (equation (3), assuming isotropic scattering), and the results are shown in Figure 6*a*. This is not a least squares fit, only a hand-chosen example. A ratio of predicted to real reflectance is shown in Figure 6*b*. The ratio illustrates the advantage of using the full theory, since the agreement with the observed spectrum is much closer than the more simplified approach discussed earlier and illustrated in Figure 3*c* and 3*d*.

Goguen [1981] has demonstrated the feasibility of the inversion concept by deriving the least squares solution to abundance of an MgO-charcoal mixture using one wavelength and many viewing geometries to solve the scattering problem. Goguen's example was limited in that the end-member scattering parameters were known and used in the mixture calculations. *Johnson et al.* [1983] applied a version of Hapke's theory to calculate reflectance spectra of mineral mixtures given the end-member spectra and noted that the procedure might be used to deconvolve abundances of the components in a spectrum of mineral mixtures if the grain size of each component and a spectrum of each of the end-members were known. The inversion idea is presented here since it is the first general mathematical presentation we are aware of which illustrates that mineral abundances may be derived from spectra of mineral mixtures when only the identity of the components are known. The accuracy of the resulting mass fractions are unknown, and it will take considerable testing by many investigators to explore the problem.

CONCLUSIONS

Kubelka-Munk (K-M) theory is limited for use in remote sensing applications, and many of the pitfalls of K-M theory can be avoided by working with apparent absorbance. The apparent absorbance has been related mathematically to transmission spectroscopy parameters, such that Gaussian features when plotted as absorption coefficient versus energy are also

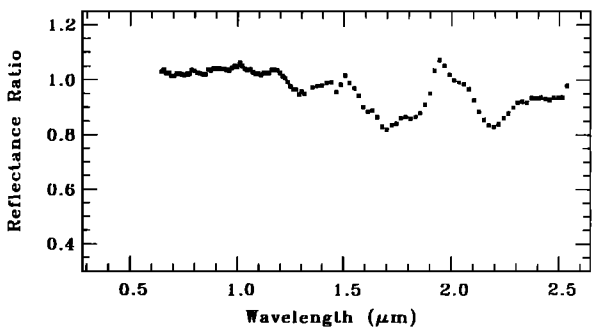

Fig. 6*b*. Ratio of predicted to measured reflectance of the two spectra in Figure 6*a*. Note that Figure 3*d* bottom is plotted on the same scale so that a full Hapke application is in considerably better agreement with the measured data.

Gaussian features in apparent absorbance versus energy but have a different amplitude and width.

An apparent continuum is a mathematical function used to isolate a particular absorption feature for analysis of a spectrum. It represents the absorption due to a different process in a specific mineral or possibly absorption from a different mineral in a multimineralic surface. Continua representing absorption processes not of interest may be removed to isolate individual absorption processes for quantitative analysis. A continuum should be removed by dividing it into the reflectance spectrum or subtracting it from the apparent absorbance.

The recently introduced scattering theories are applicable over a wider range of geologically important material than K-M theory. There is potential for deriving individual mineral abundances in a particulate surface from the scattering theories by using reflectance spectra obtained over a range of viewing geometries. In our efforts to test the equations of *Hapke* [1981] we were frustrated in not being able to find adequate data on the complex index of refraction for cosmochemically common minerals. Water ice was one exception. To our knowledge, most minerals have only had the index of refraction measured in the visible. Most geologic materials are optically anisotropic with variations in absorption coefficient along crystal axes of more than a factor of 10 [e.g., *Burns*, 1970]. However, even given such data (absorption coefficient along each crystal axis), the average absorption coefficient seen by photons in a particulate surface is not clearly determined because the mean optical path along each axis is different. However, by measuring a series of spectra of one material of different grain sizes and accurately determining the grain size distribution for each sample (e.g., by scanning electron microscope), a nonlinear least squares solution can be obtained giving both the real index of refraction and the absorption coefficient as a function of wavelength. Such analyses need to be performed for many minerals so that the data may be used in subsequent quantitative remote sensing studies.

Although the equations in the *Hapke* [1981] reflectance theory appear complex, especially compared to K-M theory and the remission function, the quantitative analysis possibilities are much more sophisticated than with K-M theory. The Hapke equations are straightforward to program on modern computers, and the brute force example of the derivation of the ice absorption coefficient in Figure 3*b* took only a fraction of a second per point on a Digital Equipment Corp. VAX 11/750 computer. For each point in that computation, the reflectance was computed by adjusting a change in the index of refraction by a factor of 2 until agreement with the reflectance was obtained to an accuracy of 0.0001. About 10–20 such computations were typically needed for convergence. This shows that rapid computations are feasible on large data sets such as might be obtained by mapping reflectance spectrometers with potential for mapping mineral abundance.

NOTATION

a a constant.
A_H directional-hemispherical reflectance.
A_p apparent absorbance.
b a constant.
$B(g)$ backscatter function which describes the opposition effect.
C_R light reflected at an index of refraction boundary.
d thickness of a plane parallel slab.
$\bar{d}$ mean optical path of a photon in a slab.
d_s average distance between grains.
D particle diameter.
D_B band depth.
D_{ν} alternative definition of band depth.
e angle of emission.
$f(r_\infty)$ Kubelka-Munk remission function.
g phase angle.
G Gaussian function.
G_0 intensity of the Gaussian function at center frequency.
$H(\mu)$ Chandrasekhar H function appearing in the reflectance equation.
i angle of incidence; also subscript denoting the ith type of particle; also subscript in summation notation.
I attenuated specific intensity.
I_0 initial specific intensity.
k volume absorption coefficient inside particle.
$\bar{k}$ average volume absorption coefficient of a multicomponent surface.
K average absorption coefficient of the medium.
$\bar{l}$ mean optical path of a photon in a particulate surface.
$\bar{l}'$ mean optical path in a single grain.
m mean number of particles encountered by photons of a particular wavelength in a surface.
M bulk density, equal to average mass per unit volume.
n real part of index of refraction; also used as an integer constant.
p physical or geometrical albedo.
$P(g)$ average particle phase function.
r reflectance.
r_C (radiance coefficient) bidirectional reflectance.
r_1 fraction of light from first order specular reflection, also used as a parameter in equations (4) and (5).
r_m fraction of light multiply scattered.
r_0 bihemispherical reflectance for isotropic scatters (Kubelka-Munk equation).
r_∞ diffuse reflectance from an infinitely thick surface.
R_B reflectance at the band center.
R_C reflectance of the continuum at the band center.
s volume scattering coefficient inside particle.
s_f first-order Fresnel reflection.
S average scattering coefficient of the medium.
S_e average surface scattering coefficient of a particle for diffuse light incident externally.
S_i average surface scattering coefficient of a particle for diffuse light incident internally.
t_m perpendicular thickness penetrated by a photon in a surface.
w single scattering albedo of a particle.
$\bar{w}$ average single scattering albedo for a surface composed of particles of different types.
W full width at half maximum of Gaussian function.
x distance a photon travels in a material.
λ wavelength.
μ cos e.
μ_0 cos i.
ϱ solid density of particle.
ϑ frequency of light.
ϑ_0 center frequency of absorption.

Acknowledgments. We thank Jay Goguen, Robert Hamilton Brown, and Paul Lucey for useful discussions. This paper has evolved

radically for its initial conception, and we would never have derived many of the results and concepts without the many generous discussions with Bruce Hapke and Carle Pieters and from the comments of the reviewers. This research was supported by NASA grant NAGW 115.

REFERENCES

Adams, J. B., Interpretation of visible and near-infrared diffuse reflectance spectra of pyroxenes and other rock-forming minerals, in *Infrared and Raman Spectroscopy of Lunar and Terrestrial Minerals,* edited by C. Karr, pp. 91–116, Academic, New York, 1975.

Burns, R. G., *Mineralogical Applications of Crystal Field Theory,* 224 pp., Cambridge University Press, Cambridge, 1970.

Chandrasekhar, S., *Radiative Transfer,* 393 pp., Dover, New York, 1960.

Charette, M. P., L. A. Soderblom, J. B. Adams, M. J. Gaffey, and T. B. McCord, Age-color relationships in the lunar highlands, *Proc. Lunar Sci. Conf., 7th,* 2579–2592, 1976.

Clark, R. N., Water frost and ice: The near-infrared spectral reflectance 0.65–2.5 μm, *J. Geophys. Res., 86,* 3087–3096, 1981*a*.

Clark, R. N., The spectral reflectance of water-mineral mixtures at low temperatures, *J. Geophys. Res., 86,* 3074–3086, 1981*b*.

Clark, R. N., Spectral properties of mixtures of montmorillonite and dark carbon grains: Implications for remote sensing minerals containing chemically and physically adsorbed water, *J. Geophys. Res., 88,* 10635–10644, 1983.

Farr, T. B., B. A. Bates, R. L. Ralph, and J. B. Adams, Effects of overlapping optical absorption bands of pyroxene and glass on the reflectance spectra of lunar soils, *Proc. Lunar Planet. Sci. Conf., 11th,* 719–729, 1980.

Goguen, J. D., A theoretical and experimental investigation of the photometric functions of particulate surfaces, Ph.D. thesis, Cornell Univ., Ithaca, N. Y., 1981.

Hapke, B., Bidirectional reflectance spectroscopy, 1; Theory, *J. Geophys. Res., 86,* 3039–3054, 1981.

Hapke, B., and E. Wells, Bidirectional reflectance spectroscopy, 2, Experiments and observations, *J. Geophys. Res., 86,* 3055–3060, 1981.

Hunt, G. R., Spectral signatures of particulate minerals, in the visible and near-infrared, *Geophysics, 42,* 501–513, 1977.

Hunt, G. R., and J. W. Salisbury, Visible and near infrared spectra of minerals and rocks; XII, Metamorphic rocks, *Mod. Geol., 5,* 219–228, 1976.

Irvine, W. M., and J. B. Pollack, Infrared optical properties of water and ice spheres, *Icarus, 8,* 324–360, 1968.

Johnson, P. E., M. O. Smith, S. Taylor-George, and J. B. Adams, A semiempirical method for analysis of the reflectance spectra of binary mineral mixtures, *J. Geophys. Res., 88,* 3557–3561, 1983.

Kortum, G., *Reflectance Spectroscopy,* 366 pp., Springer-Verlag, New York, 1969.

Lumme, K., and E. Bowell, Radiative transfer in the surfaces of atmosphereless bodies; I; Theory, *Astron. J., 86,* 1694–1704, 1981.

Lumme, K., and W. M. Irvine, Radiative transfer in the surfaces of atmosphereless bodies; III; Interpretation of lunar photometry, *Astron. J., 87,* 1076–1082, 1982.

McCord, T. B., R. N. Clark, B. R. Hawke, L. A. McFadden, P. D. Owensby, C. M. Pieters, and J. B. Adams, Moon: Near-infrared spectral reflectance, a first good look, *J. Geophys. Res., 86,* 10883–10892, 1981.

Mendell, W. W., and R. V. Morris, Band quantification in reflectance spectroscopy, *Lunar Planet. Sci., XIII,* 513–514, 1982.

Morris, R. V., S. C. Neely, and W. W. Mendell, Application of Kubelka-Munk theory of diffuse reflectance to geologic problems: The role of scattering, *Geophys. Res. Lett., 9,* 113–116, 1982.

Ockman, N., The infrared spectra and Raman-spectra of single crystals of ordinary ice, Ph.D. thesis, Univ. of Mich., Ann Arbor, 1957.

Pieters, C. M., Strength of mineral absorption features in the transmitted component of near-infrared reflected light: First results from RELAB, *J. Geophys. Res., 88,* 9534–9544, 1983.

Singer, R. B., The dark materials on Mars; II; New mineralogic interpretations from reflectance spectroscopy and petrologic implications, *Lunar Planet. Sci., XI,* 1048–1050, 1980.

Singer, R. B., Near-infrared reflectance of mineral mixtures: Systematic combinations of pyroxenes, olivine, and iron oxides, *J. Geophys. Res., 86,* 7967–7982, 1981.

Singer, R. B., Spectral evidence for the mineralogy of high-albedo soils and dust on Mars, *J. Geophys. Res., 87,* 10159–10168, 1982.

Smith, G., and R. G. J. Strens, Intervalence-transfer absorption in some silicates, oxide, and phosphate minerals, in *Physics and Chemistry of Minerals and Rocks,* edited by R. G. J. Strens, pp. 583–612, Wiley, New York, 1976.

Veverka, J., Photometry of satellite surfaces, in *Planetary Satellites,* edited by J. Burns, pp. 171–209, University of Arizona Press, Tucson, 1977.

Veverka, J., J. Goguen, S. Yang, and J. L. Elliot, How to compare the surface of Io to laboratory samples, *Icarus, 34,* 63–67, 1978.

Wendlandt, W. W., and H. G. Hecht, *Reflectance Spectroscopy,* 298 pp., Wiley-Interscience, New York, 1966.

R. N. Clark, U.S. Geological Survey, MS/964, Box 25046 Denver Federal Center, Denver, CO 80225.

T. L. Roush, Planetary Geosciences Division, Hawaii Institute of Geophysics, University of Hawaii, Honolulu, HI 96822.

(Received June 7, 1982;
revised November 14, 1983;
accepted February 15, 1984.)